Water electrolyte transport through corrugated carbon nanopores

A. Moghimi Kheirabadi* and A. Moosavi†
Department of Mechanical Engineering, Sharif University of Technology, Iran, Tehran
(Received 18 March 2014; published 14 July 2014)

We investigate the effect of wall roughness on water electrolyte transport characteristics at different temperatures through carbon nanotubes by using nonequilibrium molecular dynamics simulations. Our results reveal that shearing stress and the nominal viscosity increase with ion concentration in corrugated carbon nanotubes (CNTs), in contrast to cases in smooth CNTs. Also, the temperature increase leads to the reduction of shearing stress and the nominal viscosity at moderate degrees of wall roughness. At high degrees of wall roughness, the temperature increase will enhance radial movements and increases resistance against fluid motion. As the fluid velocity increases, the particles do not have enough time to fully adjust their positions to minimize system energy, which causes shearing stress and the nominal viscosity to increase. By increasing roughness amplitude or decreasing roughness wavelength, the shearing stress will increase. Synergistic effects of such parameters (wall roughness, velocity, ion concentration, and temperature) inside corrugated CNTs are studied and compared with each other. The molecular mechanisms are considered by investigating the radial density profile and the radial velocity profile of confined water inside modified CNT.

DOI: 10.1103/PhysRevE.90.012304 PACS number(s): 66.10.−x, 31.15.xv, 61.48.De, 68.35.Ct

I. INTRODUCTION

Due to large specific surface areas, when fluid molecules are confined in nanoenvironments, the interfacial interactions between fluid molecules and the solid wall become prominent and affect some fluid properties [1,2]. Carbon nanotubes (CNTs) have a small length scale and are widely used in various applications such as biomolecules separation [3], molecule detection [4], energy absorption [5–7], and encapsulation media for storage and transport [8]. The transport behavior of a nanofluid inside CNTs makes them appropriate for energy harvesting [9,10] and ionic separation [11,12]. Both molecular dynamics simulations [13] and experimental results [14,15] indicate that the water transport rate through CNTs is several orders of magnitude higher than that predicted from classic continuum theory.

In experimental studies, Majumder *et al.* [15] reported that liquid mass flow rates inside CNTs with a diameter of about 7 nm were four to five orders of magnitude faster than that at the macroscale and the fluid flow rate did not decrease with an increase in viscosity. Holt *et al.* [14] found that the gas flow rate inside sub-2-nm CNTs exceeds the predictions of the Knudsen diffusion model by more than an order of magnitude and water flow exceeds the prediction of continuum hydrodynamics models by more than three orders of magnitude and is comparable to flow rates extrapolated from molecular dynamics simulations. Raviv *et al.* [16] observed that the effective viscosity of water remains within a factor of 3 of its bulk value (between two curved mica surfaces), even when it is confined to films in the thickness range 0.4–3.5 nm. Li *et al.* [17] studied water films with a thickness of less than 2 nm, and they found that the water viscosity was about four orders of magnitude higher than bulk water viscosity on hydrophilic surfaces, whereas no viscosity increase was observed for hydrophobic surfaces like CNTs. Also, Major *et al.* [18] found that the measured viscosity was seven orders of magnitude greater than that of bulk water at room temperature when water was confined between two hydrophilic surfaces and the film thickness was less than 2 nm.

These experimental measurements can be sensitive to surface properties, and hence, they sometimes contradict each other. Experimental studies have tremendous difficulties in nanoenvironments, and molecular dynamics (MD) simulation as a powerful tool for predicting unique properties of nanoscale flows can be very useful [19]. In molecular dynamics simulations, Skoulidas *et al.* [20] observed that the gas transport rate inside CNTs was orders of magnitude faster than macroscales, and high transport rates in nanotubes were shown to be a result of the inherent smoothness of the nanotubes. Hummer *et al.* [13] reported that the mass flow rate of water molecules inside CNTs is much faster than that in the macroscale and fluid properties such as nominal viscosity should be reinvestigated at nanoscales. Liu *et al.* [21] found that inside a (16, 16) CNT, water viscosity was about equal to bulk water viscosity, but it nearly doubled in an (8, 8) CNT. These results were based on equilibrium molecular dynamics simulations, and such results contradict the very high transport rate of water inside CNTs observed in nonequilibrium MD simulations [13] and experiments [14].

Chen *et al.* [22] performed a nonequilibrium molecular dynamics simulation and reported that mass flow rate and CNT size have a tremendous effect on shearing stress and the nominal viscosity of water confined in the CNT. Also they reported that the radial velocity profile inside a CNT is pluglike and the nominal viscosity of water inside a (10, 10) CNT is about four orders of magnitude lower than the viscosity of bulk water.

Hanasaki and Nakatani [23] simulated water transport inside CNTs with diameters from (6, 6) to (20, 20) and reported that at very high transport speed, the velocity profile is pluglike. Liu and Chen [24] studied water electrolyte solution transport in silica and carbon tortuous nanotubes and reported

*moghimi@mech.sharif.edu
†Corresponding author: moosavi@sharif.edu

that ion transport is much faster than water molecule transport inside such nanoenvironments. Zhao *et al.* [25] carried out a nonequilibrium molecular dynamics (NEMD) simulation on an (18, 18) nanotube and reported that by increasing ion concentration of the water electrolyte solution, shearing stress and the nominal viscosity increase. Also they found that by varying the properties of the liquid phase and solid phase, liquid flow rate, and nanotube size, the energy absorption characteristics of a nanofluidic device might be adjusted. Xu *et al.* [26] studied thermally responsive transport resistance of liquids in model carbon nanotubes as a function of the nanopore size, the transport rate, and the liquid properties. They found that both the effective shear stress and the nominal viscosity decrease with the increase of temperature, and the temperature effect is coupled with other nonthermal factors. Recently, we have studied [27] and validated the effect of ion concentration, nanotube size, and the fluid temperature on the fluid transport resistance inside smooth nanopores [22], and we have found the effects of such parameters on the mean shearing stress cannot be superposed.

Jabbarzadeh *et al.* [28] investigated molecularly thin liquid films of alkanes in extreme conditions between two sinusoidal walls, and they found that the relative size of the fluid molecules and wall roughness determines the slip or nonslip boundary conditions. Mittal and Hummer [29] studied the effects of nanoscopic roughness on the interfacial free energy of water confined between two solid surfaces and found that interfacial free energy near the rough surface is much higher compared to that at the smooth surface. Joseph and Aluru [30] performed a molecular dynamics simulation and found that the roughness in the tube walls causes strong a hydrogen-bonding network and no significant flow enhancement is attained in rough tubes. Xu *et al.* [31] studied the effect of wall roughness on the transport resistance of water molecules inside modified CNTs and found that both the effective shearing stress and nominal viscosity increase with the increase of amplitude or decrease of the wavelength of the roughness.

Most previous molecular dynamics simulations of nanofluidics were focused on ideally smooth nanochannels. However, many nanoporous materials have prominent wall surface roughness [30,31]. The effects of simultaneous changes of mass flow rate, ion concentration, and the fluid temperature on the water electrolyte transport inside modified CNTs is unknown and should be studied to better understand transport phenomena in nanoscales.

In the present study a (20, 20) CNT is considered, and the tube wall is perturbed with a sinusoidal surface morphology [31]. A NEMD simulation is carried out to explore the effect of mean flow velocity, wall roughness, fluid temperature, and ion concentration on the shearing stress and the nominal viscosity. The effective shearing stress encountered by water molecules during transport is employed to characterize the solid-water electrolyte solution interactions [22]. Also the simultaneous effects of these parameters (ion concentration, temperature, and wall roughness) on the fluid transport inside a modified CNT are investigated. The molecular mechanisms that affect the fluid transport characteristics are explored through the study of the radial density profile (RDP) and radial velocity profile (RVP) of a confined liquid solution.

TABLE I. Electrical charge of all particles in this simulation [22,25,26].

q_{Na^+}	q_{Cl^-}	q_O	q_H	q_C
$1.0e$	$-1.0e$	$-0.834e$	$+0.417e$	$0.0e$

II. MOLECULAR DYNAMICS SIMULATION

For the water molecules, the transferable intermolecular potential three-point (TIP3P) model [32] is adopted, and the potential function between all particles is as follows:

$$V = \sum \frac{kq_i q_j}{r_{ij}} + \sum 4\varepsilon\left[\left(\frac{\sigma}{r}\right)^{12} - \left(\frac{\sigma}{r}\right)^{6}\right]. \quad (1)$$

The first term on the right hand side of Eq. (1) is the Columbic potential, the derivative of which is the electrostatic interaction among electropolar atoms and ions (hydrogen, oxygen, carbon, Na^+, and Cl^- ions). Table I shows the electrical charge of each particle (Na^+, Cl^-, O, C, and H).

The second term on the right hand side of Eq. (1) is Lennard-Jones potential, the derivative of which is the van der Waals (vdW) interaction among all particles except hydrogen atoms. The Lennard-Jones potential between hydrogen and the other particles in the system is considered to be zero [25]. Table II indicates the Lennard-Jones parameters among all particles in this simulation.

NEMDs were performed to investigate molecular transport of a water electrolyte inside modified (20, 20) CNTs. LAMMPS was used to carry out these simulations [33]. As shown in Fig. 1, a model (20, 20) CNT which is perturbed with a sinusoidal wall roughness [31] is considered, and the water electrolyte solution transport inside such a modified nanochannel is explored. The local radius at distance z is described as $R = R_0 + A\sin(2\pi z/\lambda)$, where R_0 is the radius of the smooth baseline, A is the roughness amplitude, and λ is the roughness wavelength [31]. The roughness amplitude is considered to be less than 0.5 nm [34–36]. The nanotube length is taken to be 300 Å (nanotube length to diameter ratio is considered to be large enough), and several NEMD simulations were carried out and show that by increasing the nanotube length from 300 Å, the results do not vary. As shown

TABLE II. The Lennard-Jones potential parameters among all particles in this simulation [22,25,31]. The effective values of σ and ε are calculated from those for the homatomic pairs using the Lorentz-Berthelot mixing rules.

ε		σ	
ε_{OC}	0.105 kcal/mol	σ_{OC}	3.1905 Å
ε_{OO}	0.1521 kcal/mol	σ_{OO}	3.5365 Å
ε_{ONa^+}	0.4324 kcal/mol	σ_{ONa^+}	3.8057 Å
ε_{OCl^-}	0.2806 kcal/mol	σ_{OCl^-}	3.777 Å
$\varepsilon_{Na^+Na^+}$	0.1301 kcal/mol	$\sigma_{Na^+Na^+}$	2.3502 Å
$\varepsilon_{Na^+Cl^-}$	0.114 kcal/mol	$\sigma_{Na^+Cl^-}$	3.375 Å
ε_{Na^+C}	0.125 kcal/mol	σ_{Na^+C}	2.823 Å
ε_{Cl^-C}	0.109 kcal/mol	σ_{Cl^-C}	3.848 Å
$\varepsilon_{Cl^-Cl^-}$	0.10 kcal/mol	$\sigma_{Cl^-Cl^-}$	4.40 Å

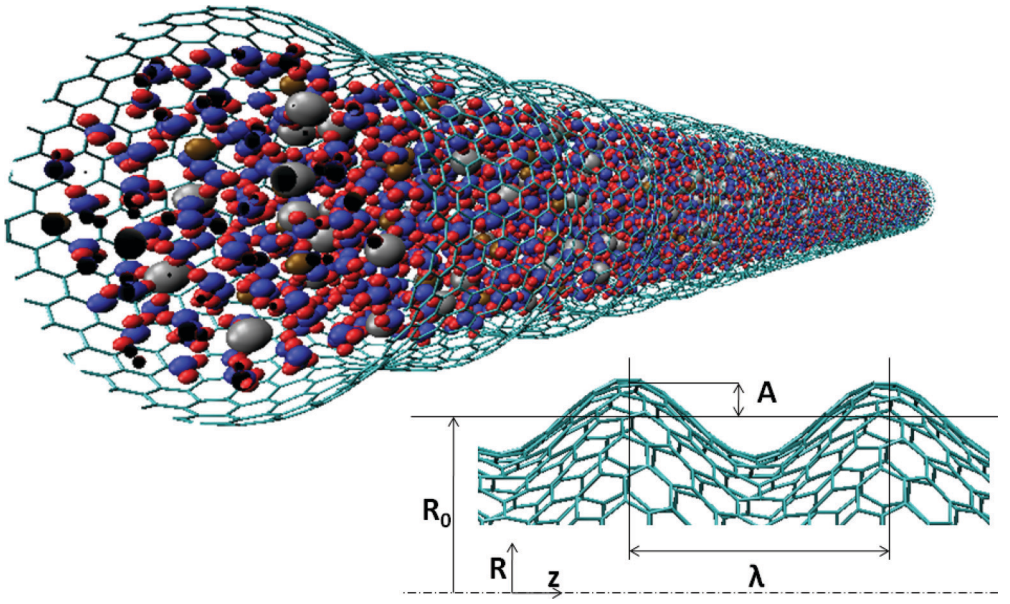

FIG. 1. (Color online) Distribution of 20% water electrolyte solution inside a modified (20, 20) CNT [31] after initial relaxation. The roughness amplitude is $A/R_0 = 0.06$, and the roughness wavelength is $\lambda/R_0 = 1.0$. The blue spheres stand for oxygen atoms, the red spheres stand for hydrogen atoms, the brown spheres stand for sodium ions, and the gray balls stand for chloride ions.

in Fig. 2, in order to mimic an infinitely long nanochannel, a periodic boundary condition is applied along the nanochannel axis. The number of particles (water molecules and ions) inside the corrugated CNT was chosen such that the solution density inside the occupied volume is equal to that at macroscales. A C++ code was developed to generate a modified nanopore with the desired roughness parameters, and all particles were randomly placed inside such a modified nanoenvironment. At high pressure gradients, the flexibility of the CNT does not have significant effects on the free energy of molecules and ions [37], and the modified CNT can be considered as a rigid wall [22,25,31]. In addition, if the wall is flexible, during a MD simulation, the roughness profile may deviate from the expected value, which makes it difficult to correlate amplitude and wavelength values with nanofluidic transport characteristics [31]. In the present study, the roughness parameters are considered to be within moderate ranges [31], such that the tube wall roughness is relatively stable.

The cutoff radius for the Lennard-Jones and the real-space part of Coulomb interactions is considered to be 10 Å [22]. The long-range electrostatic interactions are calculated by using the particle-particle particle-mesh (PPPM) method [25] with a root mean accuracy of 10^{-4}. The neighbor skin distance is set to be 5 Å. The time step in this study is chosen to be 1 fs. During simulations, the temperature of the fluid was kept at the desired value by using a Nose-Hoover thermostat with a time constant of 0.1 ps. The SHAKE algorithm is used to constrain bonds and angles within water molecules. By using an *NVT* (canonical) ensemble, the initial configuration of water molecules and ions is relaxed for 100 ps. As shown in Fig. 2, after the initial relaxation, the fluid particles show a harmonious distribution with respect to the CNT wall. The nanofluidic transport through confined nanochannels is typically a nonequilibrium process, and a NEMD simulation is usually performed to observe the phenomenon in such nanofluidic systems. When the system is fully relaxed and the energy is minimized, a constant external acceleration is applied to each particle along the nanotube axis to reach the desired mass flux. During this step, an *NVT* ensemble is used, and the mean flow velocity is subtracted from the axial component of all fluid particles to avoid artificial heating. When the average transport velocity of all particles reaches 300 m/s, the external force is removed, and the liquid decelerates freely. An *NVE* ensemble is employed to monitor mean fluid velocity reduction. By using the Newton's second law, the mean shearing stress at the liquid-solid interface is defined as $\sum m_i a/S$, where $\sum m_i$ is the total mass of fluid inside the CNT (including water molecules and electrolyte ions), a is the

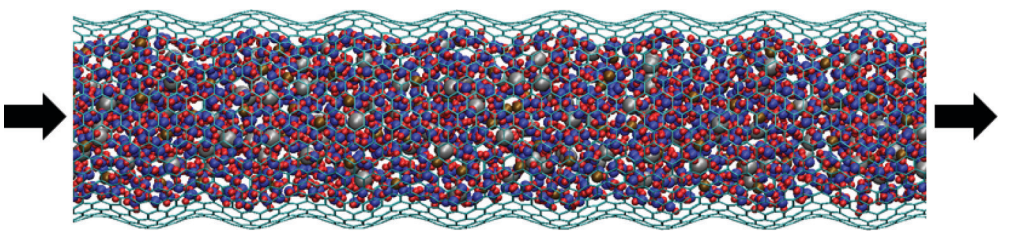

FIG. 2. (Color online) A 20% water electrolyte solution inside a modified (20, 20) CNT. The roughness amplitude is $A/R_0 = 0.06$, and the roughness wavelength is $\lambda/R_0 = 1.0$. A periodical boundary condition is applied along the CNT axis.

mean deceleration of particles, and S is the surface area of a rough CNT. Although the fluid flow inside a modified CNT is not continuous, we define a nominal viscosity μ which characterize the fluid property resulting from solid-liquid interface interactions [22,25,26,31]. The nominal viscosity is dependent on the fluid transport characteristics and is obtained from a comparison of pressure drop at nano- and macroscales. Therefore, the nominal viscosity is assessed as $\tau R_0/4v$ [22], where τ is the mean shearing stress, R_0 is the nanotube base radius, and v is the mean flow velocity. This equation is based on continuum theory and can be used for the purpose of self-comparison only; however, it can be used for complex flows [38,39].

III. RESULTS AND DISCUSSION

In order to understand molecular mechanisms inside nanoenvironments, the RDP of confined water inside modified CNTs with different degrees of roughness is considered. Figure 3 depicts the RDP of confined pure water inside a rough (20, 20) CNT when the temperature is kept at 298 K. Radial density profiles have fluctuations which indicate the annular layer structure of molecular ordering, and this is consistent with previous studies [31]. As shown, the roughness parameters affect the RDP of confined water. The maximum density near the tube wall is referred to as the first solvation shell (FSS), and its distance to the CNT wall is referred to as the equilibrium distance.

When the roughness wavelength is constant, by increasing the roughness amplitude A/R_0, the water molecules are trapped in wall cavities, and in these cases the RDP has two peaks near the tube wall. In the case of $A/R_0 = 0.04$, by decreasing the roughness wavelength λ/R_0, the water molecules get closer to the tube center, and the FSS will increase. When $A/R_0 = 0.06$, when λ decreases from $2.0R_0$ to $1.0R_0$, the magnitude of the FSS (first peak) decreases, and the equilibrium distance increases. As shown in Fig. 3, the density of confined pure water inside modified nanopores has fluctuations around its average density (998 kg/m^3 based on numerical calculations), which is equal to that at macroscales where the temperature is 298 K and the pressure is 1.0 bar.

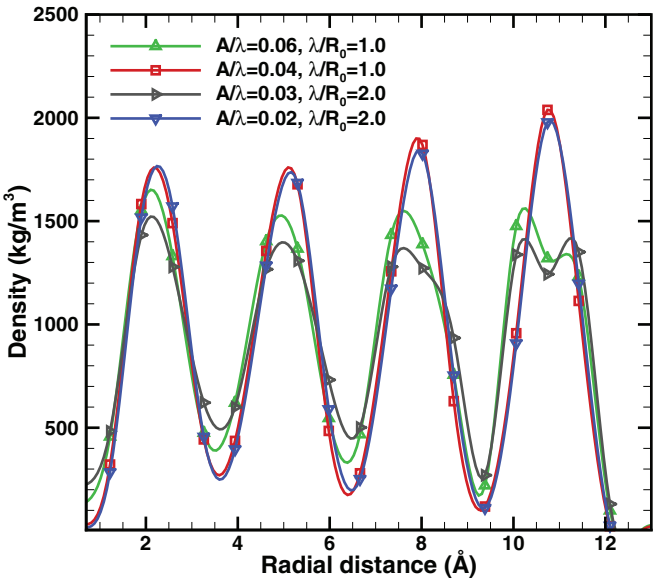

FIG. 3. (Color online) RDP of pure water inside modified CNTs with different relative roughness parameters. The temperature is kept at 298 K. The roughness parameters affect the FSS location and push that toward the tube's center.

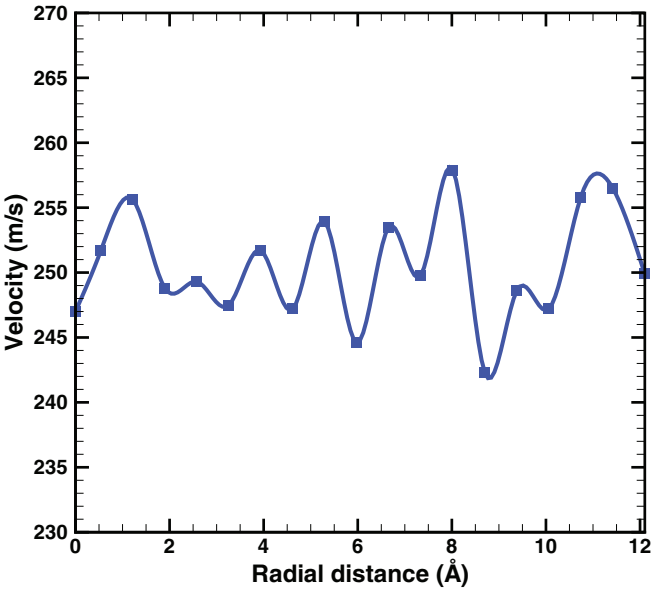

FIG. 4. (Color online) RVP of pure water confined inside a (20, 20) corrugated nanopore with $A/R_0 = 0.06$ and $\lambda/R_0 = 2$. The temperature is kept at 298 K. The mean fluid velocity is 250 m/s, and the RVP is pluglike.

Figure 4 shows the mean axial velocity at different radial distances when the mean fluid velocity along the nanotube axis is about 250 m/s. At high velocities, the RVP is nearly constant, with small fluctuations around its mean value. As shown, the RVP is a plug-flow profile, and it is consistent with the other numerical investigations [22,23]. The CNTs are hydrophobic in nature, and the water molecules can slip freely against the nanotube wall. Also the water molecules have strong hydrogen bonds among each other. As a result, when the water molecules are transported through the CNT, they attract each other and form bulk flow.

Figure 5 shows the mean shearing stress for a (20, 20) CNT with different degrees of wall roughness. The wall roughness ratio, which represents the roughness amplitude to roughness wavelength ratio (A/λ), is a parameter that describes the tube wall effective roughness.

As shown in Fig. 5, the mean shearing stress increases nonlinearly with both wall roughness ratio and the mean fluid velocity, and the effect of mean fluid velocity is more prominent in tubes with higher degrees of roughness. The rough bulges on the tube wall affect the water transport inside the CNT and perturb the uniform axial flow, which enhances the radial movements of particles near the tube wall [30]. By increasing the effective roughness (increasing A/R_0 or decreasing λ/R_0), the radial movement will become more prominent, and the particles near the tube center are also affected. Increasing the radial movement of water molecules will enhance the collision possibility of fluid particles with the

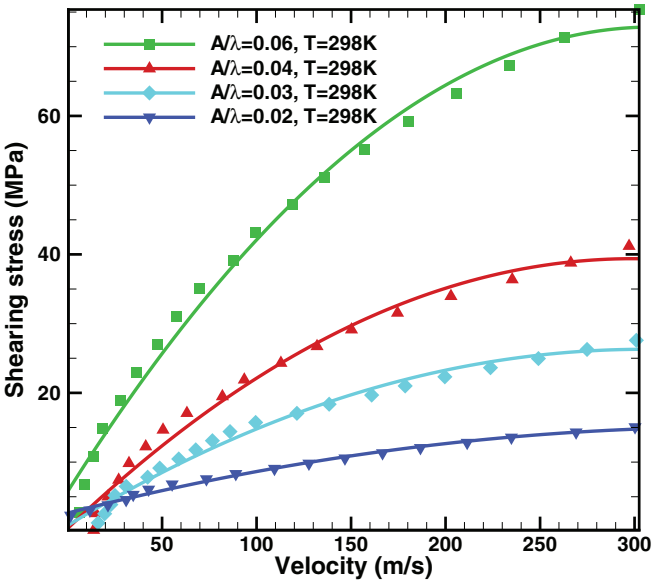

FIG. 5. (Color online) The mean shearing stress at different relative roughness parameters. The temperature is 298 K, and the ion concentration is 0.0 wt %.As the tube roughness amplitude to wavelength increases, the shearing stress will increase. By increasing fluid flow velocity, the mean shearing stress increases.

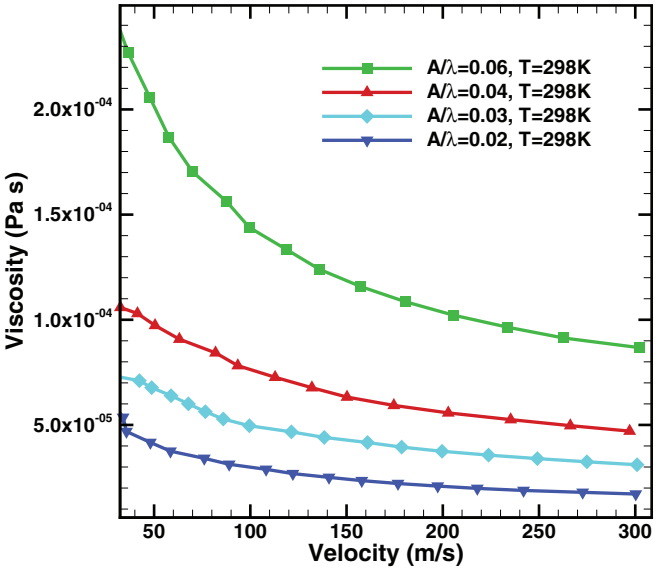

FIG. 6. (Color online) The nominal viscosity at different relative roughness parameters. The temperature is 298 K, and the ion concentration is 0.0 wt %. As the tube roughness amplitude to wavelength increases, the nominal viscosity will increase. By increasing fluid flow velocity, the nominal viscosity decreases and is asymptotic to a constant value.

corrugated tube wall, and therefore, water transport resistance in the axial direction (shearing stress) will increase.

The shearing stress is also dependent on the mass flow rate, and by increasing the effective wall roughness, this dependency will increase more strongly (Fig. 5). By increasing mean velocity v, as the fluid particles move along the CNT, there is not sufficient time for the water molecules to fully adjust their positions to minimize system free energy. Therefore, the distance between wall atoms and the water molecules can be less than the van der Waals equilibrium distance, which leads to higher shearing stress [22,25,26]. Also by increasing wall effective roughness, more water molecules are trapped in the wall cavities, and by increasing fluid velocity, such molecules do not have enough time to adjust their position to minimize system free energy; therefore, in these cases the shearing stress is more dependent on the mass flow rate. Figure 6 depicts the nominal viscosity of pure water inside a modified CNT at different wall roughnesses. The nominal viscosity is dependent on both shearing stress τ and the mean fluid velocity v and is expressed as $\tau R_0/4v$. By increasing wall effective roughness, the shearing stress increases, and as a result, the nominal viscosity increases. By increasing the mean fluid velocity, the rate of increasing shearing stress is less than mean fluid velocity, and therefore, the nominal viscosity decreases and at higher velocities asymptotes to a constant value. At higher velocities, the mass flow rate effects are negligible, and the temperature and ion concentration effects on the nominal viscosity can be further analyzed.

In order to investigate the effect of ion concentration on shearing stress and nominal viscosity through corrugated nanopores, the RDP of a water electrolyte solution at different concentrations is explored. Figure 7 indicates the RDP of a saltwater solution inside a corrugated CNT. As the ion concentration is raised, the first solvation shell density increases and goes toward the tube center. The distributed electrical field arising from Na^+ and Cl^- ions affects nanofluidic behavior, and such variations may be significantly different than those associated with pure water. The Na^+ and Cl^- ions intensify the Coulomb interactions with the polar water molecules. These ions agglomerate water molecules around them, so as to make such flow more coherent and attract the first solvation

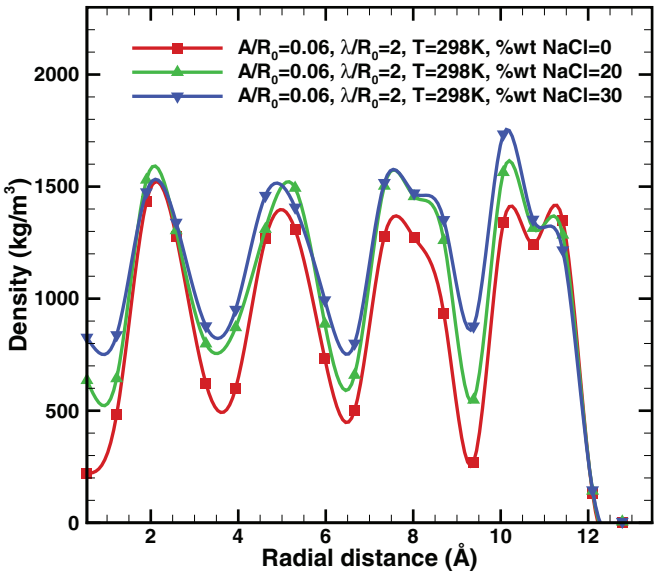

FIG. 7. (Color online) RDP of saltwater solution inside a corrugated (20, 20) CNT with roughness parameters $A/R_0 = 0.06$ and $\lambda/R_0 = 2$ at $T = 298$ K. When the ion concentration increases, the FSS moves away from the tube wall, and the maximum density increases.

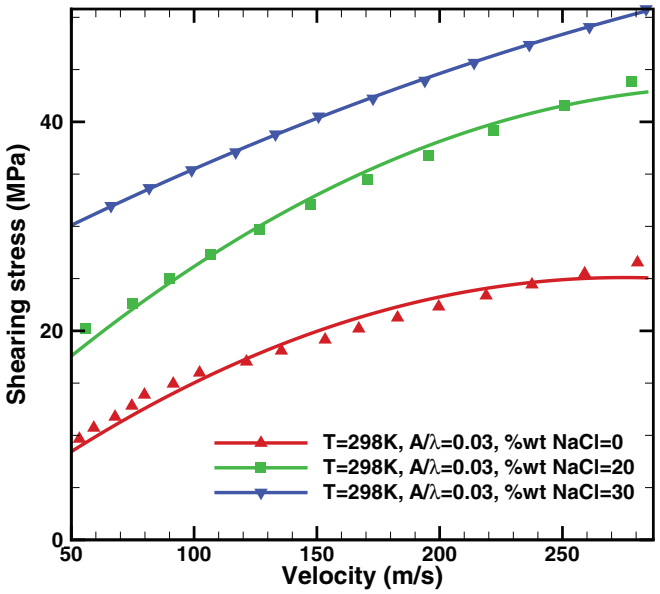

FIG. 8. (Color online) The mean shearing stress at different NaCl concentrations inside a corrugated (20, 20) CNT. The temperature is 298 K, and the ion wall roughness parameters are $A/R_0 = 0.06$ and $\lambda/R_0 = 2.0$. As ion concentration increases, the shearing stress will increase. By increasing fluid flow velocity, the mean shearing stress increases with mean velocity as in pure water.

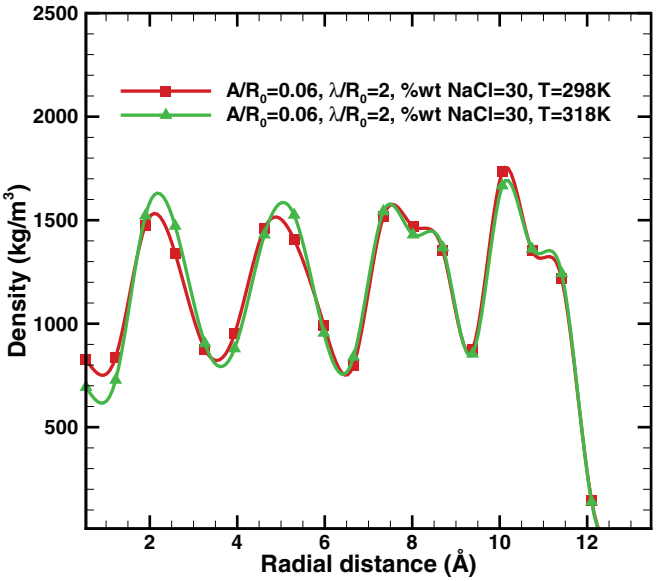

FIG. 10. (Color online) RDP of 30 wt % saltwater solution inside corrugated a (20, 20) CNT with roughness parameters $A/R_0 = 0.06$ and $\lambda/R_0 = 2$ at two different temperatures. When temperature increases, the FSS is attracted to the tube wall, and the maximum density decreases.

shell to the tube center. As in the pure water cases, the RDP has fluctuations which indicate the annular layer structure of molecule and ion ordering [25].

As seen in Figs. 8 and 9, the mean shearing stress and the nominal viscosity increase as more ions are added to the pure water. When the CNT wall is smooth, the shearing stress and the nominal viscosity decrease with NaCl concentration [25]. When the CNT wall is corrugated, some Na^+ and Cl^- ions are trapped in the wall cavities. Electrical interactions between trapped ions and the particles near the tube wall make it harder for polar particles to slip along the nanotube axis, which turns the CNT wall into a hydrophilic material. On the other hand, by raising the ion concentration, the possibility of a collision between ions and the extrusions on the tube wall increases, and as a result, the radial movement of agglomerated ions will be enhanced. The axial flow is perturbed, and therefore, the shearing stress and nominal viscosity increase.

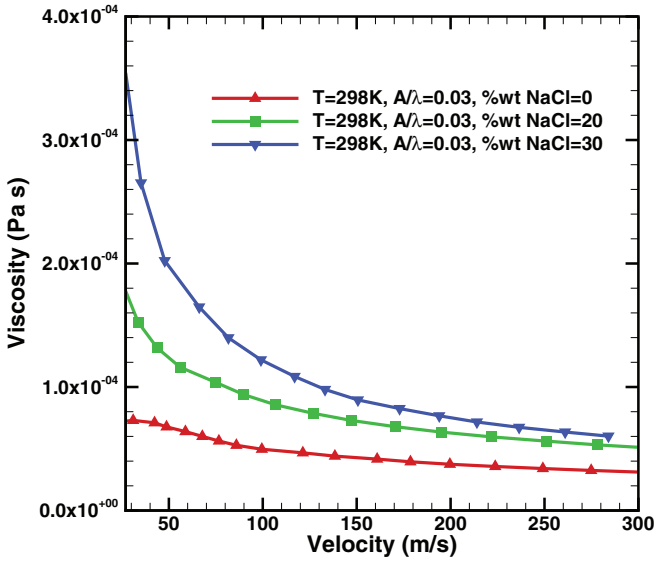

FIG. 9. (Color online) The nominal viscosity at different NaCl concentrations inside a corrugated (20, 20) CNT. The temperature is 298 K, and the wall roughness parameters are $A/R_0 = 0.06$ and $\lambda/R_0 = 2.0$. As ion concentration increases, the nominal viscosity will increase. By increasing fluid flow velocity, the nominal viscosity decreases with mean velocity as in pure water.

Also the nominal viscosity and the shearing stress depend on the mean fluid velocity, and their dependency is as for the pure water cases discussed earlier. The temperature of the saltwater solution also changes the molecular structure, and it is expected to affect shearing stress inside the modified CNT [31]. In order to investigate the effect of temperature on water electrolyte transport inside corrugated nanopores, two different cases are considered. Figure 10 depicts radial density profiles of a confined solution in a (20, 20) modified CNT. As can be seen, the fluctuations indicate the annular layer structure of water molecules and ions inside the corrugated CNT. Both the amplitude of the first solvation shell and the equilibrium distance are higher in the case of $T = 298$ K than those in the case of $T = 318$ K.

Increasing fluid temperature causes thermal movements to be faster, and as a result, due to the vdW and the Coulomb interactions, the average intermolecular distance increases, and the FSS is attracted to the tube wall. This behavior occurs as FSS variations with the temperature increase in smooth CNTs [26,27]. Figure 11 depicts the shearing stress and nominal viscosity profiles when the temperature is raised from 298 to 318 K. As can be seen, as the solution temperature

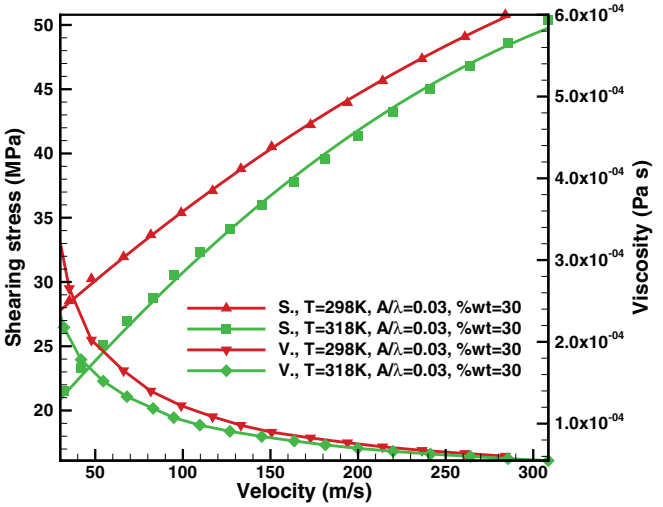

FIG. 11. (Color online) The nominal viscosity and the shearing stress of a 30 wt % saltwater solution at two different temperatures inside a corrugated (20, 20) CNT. The wall roughness parameters are $A/R_0 = 0.06$ and $\lambda/R_0 = 2.0$. As the fluid temperature increases, the nominal viscosity and shearing stress will decrease. By increasing fluid flow velocity, the shearing stress and the nominal viscosity decreases with mean velocity as in pure water in CNT.

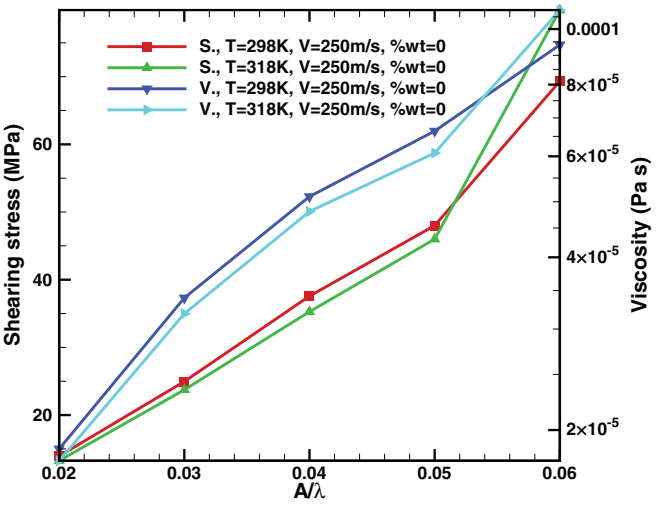

FIG. 12. (Color online) The shearing stress and the nominal viscosity of pure water at different degrees of wall roughness inside a modified (20, 20) CNT. The mean fluid velocity is 250 m/s. The shearing stress and the nominal viscosity increase as wall roughness increases. These two parameters decrease with increasing fluid temperature except at high degrees of wall roughness.

increases, the mean shearing stress and the nominal viscosity decrease.

As discussed earlier, as temperature increases, both the FSS density and the equilibrium distance decrease, which implies weaker solid wall-fluid intermolecular interactions. In addition under such a condition, the radial confinement effect imposed on solution particles is less severe. Therefore, the axial component of the velocity of water molecules and ions is relatively more prominent, which causes smaller transport resistance, and as a result, the mean shearing stress and the nominal viscosity become less than those at lower temperatures [26].

Figure 12 explores the effect of fluid temperature on the shearing stress and the nominal viscosity at different degrees of wall roughness. As can be seen, at low degrees of wall roughness, the shearing stress and the nominal viscosity decrease as temperature rises. By increasing the fluid temperature, thermal movements of water molecules will become faster.

When water flows through a CNT with high degrees of wall roughness, the possibility of collision between particles and the rough extrusions on the CNT wall increases due to thermal movements, and as a result, resistance against fluid motion will become stronger. Therefore, the shearing stress and the nominal viscosity will become higher. Also by increasing wall roughness the relative dimensionless shear difference $(\tau_{298}\text{-}\tau_{318})/\tau_{298}$ decreases, and at some wall roughness its sign will change.

Figure 13 indicates the shearing stress of a water electrolyte solution inside modified CNTs at different ion concentrations. As shown, shearing stress increases with ion concentration and wall roughness, and the rate of increasing is more severe at higher salt concentrations. Adding ions to the pure water changes the molecular structure and affects the nanofluidic transport characteristics. Therefore, by adding a certain amount of salt to pure water, the nanofluidic transport behavior inside corrugated nanopores can be adjusted, and such characteristics can be used to better design nanoelectromechanical systems.

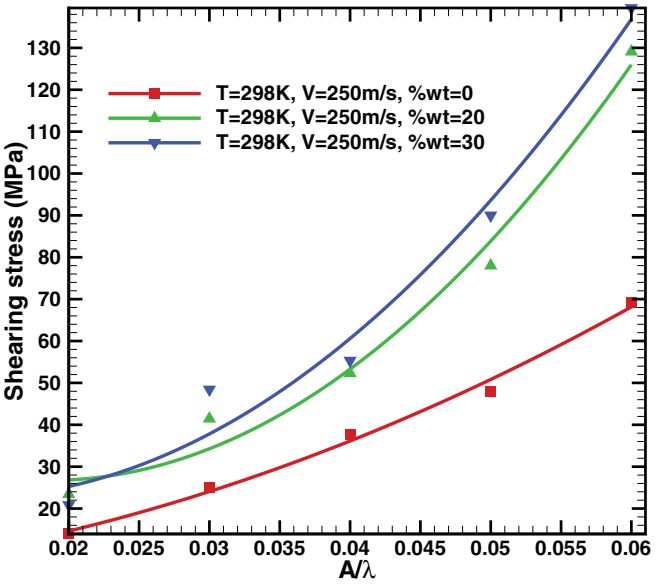

FIG. 13. (Color online) The mean shearing stress of a water electrolyte solution at different degrees of wall roughness inside a modified (20, 20) CNT. The mean fluid velocity is 250 m/s. The shearing stress increases with ion concentration and wall roughness. The rate of increase of the shearing stress is more severe at higher ion concentrations.

IV. CONCLUSION

In summary, the transport behavior of a saltwater solution inside a modified (20, 20) CNT was investigated using a nonequilibrium molecular dynamics simulation. The results show that the shearing stress and nominal viscosity inside corrugated CNTs are dependent on mass flow rate, roughness amplitude, roughness wavelength, salt concentration, and solution temperature. The detailed analysis of simulations showed that wall roughness has considerable effects on the water electrolyte transport properties. Increasing the effective wall roughness leads to higher shearing stress and nominal viscosity, which is consistent with previous numerical and experimental investigations. Unlike water electrolyte motion through smooth CNTs, increasing ion concentration inside modified CNTs increases shearing stress and nominal viscosity. At moderate degrees of wall roughness, by increasing fluid temperature, the shearing stress and the nominal viscosity decrease, and these phenomena are similar to fluid transport inside smooth CNTs. In the cases of higher degrees of wall roughness, increasing the fluid temperature perturbs the axial flow and enhances resistance against fluid motion. Simultaneous effects of ion concentration, temperature, and wall roughness show that by adding more ions to pure water, the shearing stress will increase more severely with wall roughness. Increasing the fluid temperature does not have a strong effect on shearing stress at low degrees of wall roughness. By increasing the effective wall roughness, the temperature effect will become more prominent.

The present study may provide several applications for designing nanoelectromechanical systems by adjusting fluid motion resistance and the energy absorption of the system.

[1] W. Sparreboom, A. Vandenberg, and J. C. T. Eijkel, Nat. Nanotechnol. **4**, 713 (2009).
[2] L. Bocquet and E. Charlaix, Chem. Soc. Rev. **39**, 1073 (2010).
[3] K. B. Jirage, J. C. Hulteen, and C. R. Martin, Science **278**, 655 (1997).
[4] D. W. Deamer and M. Akeson, Trends Biotechnol. **18**, 147 (2000).
[5] X. Chen, F. B. Surani, X. Kong, V. K. Punyamurtula, and Y. Qiao, Appl. Phys. Lett. **89**, 241918 (2006).
[6] L. Liu, Y. Qiao, and X. Chen, Appl. Phys. Lett. **92**, 101927 (2008).
[7] Y. Qiao, G. Cao, and X. Chen, J. Am. Chem. Soc. **129**, 2355 (2007).
[8] A. Kalra, S. Garde, and G. Hummer, Proc. Natl. Acad. Sci. USA **100**, 10175 (2003).
[9] F. H. J. van der Heyden, D. J. Bonthuis, D. Stein, C. Meyer, and C. Dekker, Nano Lett. **7**, 1022 (2007).
[10] Y. Ren and D. Stein, Nanotechnology **19**, 195707 (2008).
[11] I. Vlassiouk, S. Smirnov, and Z. Siwy, Nano Lett. **8**, 1978 (2008).
[12] X. Gong, J. Li, K. Xu, J. Wang, and H. J. Yang, Am. Chem. Soc. **132**, 1873 (2010).
[13] G. Hummer, J. G. Rasalah, and J. P. Noworyta, Nature (London) **414**, 188 (2001).
[14] J. K. Holt, H. G. Park, Y. M. Wang, M. Stadermann, A. B. Artyukhin, C. P. Grigoropoulos, A. Noy, and O. Bakajin, Science **312**, 1034 (2006).
[15] M. Majumder, N. Chopra, R. Andrews, and B. J. Hinds, Nature (London) **438**, 44 (2005).
[16] U. Raviv, P. Laurat, and J. Klein, Nature (London) **413**, 51 (2001).
[17] T.-D. Li, J. Gao, R. Szoszkiewicz, U. Landman, and E. Riedo, Phys. Rev. B **75**, 115415 (2007).
[18] R. C. Major, J. E. Houston, M. J. McGrath, J. I. Siepmann, and X.-Y. Zhu, Phys. Rev. Lett. **96**, 177803 (2006).
[19] A. I. Kolesnikov, J. M. Zanotti, C. K. Loong, P. Thiyagarajan, A. P. Moravsky, R. O. Loutfy, and C. J. Burnham, Phys. Rev. Lett. **93**, 035503 (2004).
[20] A. I. Skoulidas, D. M. Ackerman, J. K. Johnson, and D. S. Sholl, Phys. Rev. Lett. **89**, 185901 (2002).
[21] Y. Liu, Q. Wang, T. Wu, and L. Zhang, J. Chem. Phys. **123**, 234701 (2005).
[22] X. Chen, G. Cao, A. Han, V. K. Punyamurtula, L. Liu, P. J. Culligan, T. Kim, and Y. Qiao, Nano Lett. **8**, 2988 (2008).
[23] I. Hanasaki and A. Nakatani, J. Chem. Phys. **124**, 144708 (2006).
[24] A. Han and Y. Qiao, Chem. Lett. **36**, 882 (2007).
[25] J. Zhao, Y. Qiao, P. J. Culligan, and X. Chen, J. Comput. Theor. Nanosci. **7**, 379 (2010).
[26] B. Xu, B. Wang, T. Park, Y. Qiao, Q. Zhou, and X. Chen, J. Chem. Phys. **136**, 184701 (2012).
[27] A. Moghimi-Kheirabadi, A. Moosavi, and A. M. Akbarzadeh, J. Phys. D **47**, 065304 (2014).
[28] A. Jabbarzadeh, J. D. Atkinson, and R. I. Tanner, Phys. Rev. E **61**, 690 (2000).
[29] J. Mittal and G. Hummer, Faraday Discuss. **146**, 341 (2010).
[30] S. Joseph and N. R. Aluru, Nano Lett. **8**, 452 (2008).
[31] B. Xu, Y. Li, T. Park, and X. Chen, J. Chem. Phys. **135**, 144703 (2011).
[32] W. L. Jorgensen, J. Chandrasekhar, J. D. Madura, R. W. Impey, and M. L. Klein, J. Chem. Phys. **79**, 926 (1983).
[33] S. Plimpton, J. Comput. Phys. **117**, 1 (1995).
[34] A. Fasolino, J. H. Los, and M. Katsnelson, Nat. Mater. **6**, 858 (2007).
[35] J. C. Meyer, A. K. Geim, M. I. Katsnelson, K. S. Novoselov, T. J. Booth, and S. Roth, Nature (London) **446**, 60 (2007).
[36] N. Abedpour, M. Neek-Amal, R. Asgari, F. Shahbazi, N. Nafari, and M. R. Tabar, Phys. Rev. B **76**, 195407 (2007).
[37] S. Andreev, D. Reichman, and G. Hummer, J. Chem. Phys. **123**, 194502 (2005).
[38] J. P. Rothstein and G. H. McKinley, J. Non-Newtonian Fluid Mech. **86**, 61 (1999).
[39] D. Semwogerere, J. F. Morris, and E. R. Weeks, J. Fluid Mech. **581**, 437 (2007).